Intestinal wall-adhesive hydrogel to study therapeutic treatment of inflammatory bowel disease

Tae Young Kim

Department of Medical Science

The Graduate School, Yonsei University

Intestinal wall-adhesive hydrogel to study therapeutic treatment of inflammatory bowel disease

Directed by Professor Hak-Joon Sung

The Master's Thesis
the Department of Medical Science,
the Graduate School of Yonsei University
in partial fulfillment of the requirements for the degree of
Master of Medical Science

Tae Young Kim

December 2020

This certifies that the Master's Thesis of
Taeyoung Kim is approved.

_____

Thesis Supervisor: Hak-Joon Sung

_____

Thesis Committee Member#1: Jong-Chul Park

_____

Thesis Committee Member#2: Chang Soo Kim

The Graduate School
Yonsei University

December 2020

ACKNOWLEDGEMENTS

I completed my two-year master's program and submitted my thesis. I know that this margin given to express my gratitude by borrowing a few letters like this, but in the past two years of graduate school life, I know that I have awakened and taught a lot of things beyond the framework of 'learning'. I would like to express my gratitude by borrowing paper. First of all, I would like to express my deepest gratitude to Professor Hak-Joon Sung, my supervisor, who gave me many opportunities and support as well as academic teaching, and who sometimes criticized and rebuked me and guided me correctly to move forward. In addition, I sincerely thank Professor Jong-Chul Park and Chang Soo Kim for taking time to review the thesis and giving warm encouragement and advice in the midst of a busy schedule. From the beginning of my graduate school life to now, I sincerely thank Dr. Young Min Shin, who has always led me to the path of a researcher with a passionate attitude, who always cherished me so that I could finish my degree course well and served as a big support for my graduate life. Thanks to the members of the Regenerative Biomedical Engineering Lab. Finally, I bow my head to my deep thanks to my unparalleled parents who supported me during my master's life and always watched and trusted me silently until this moment. And I would like to express my gratitude to my companion, Seo Jeong, who has always supported me.

TABLE OF CONTENTS

LIST OF FIGURES

LIST OF TABLES

ABSTRACT

Intestinal wall-adhesive hydrogel to study therapeutic treatment of inflammatory bowel disease

Tae Young Kim

Department of Medical Science

The Graduate School, Yonsei University

(Directed by Professor Hak-Joon Sung)

Inflammatory bowel disease (IBD) is defined as pathogenesis in the intestine in a form of ulcerative colitis, Crohn's disease, etc. The number of IBD patients has recently increased rapidly majorly due to western diet and lifestyle. Because current treatment methods of IBD in the field are limited in targeting specific location and accompanying side effects such as vomiting, burping and chest pain occur. Hence, an unmet need remains in suggesting new perspective of drug delivery system to overcome these problems. Here, as an effort to develop an intestinal wall-adhesive, target specific peptide-conjugated hydrogel as a means of drug delivery, we synthesize mPEG-PCL (methoxy poly (ethylene glycol)-block-poly(ε-caprolactone)). The mPEG-PCL exhibits molecule weight

of 3,200-3,500 g/mol, and its sol-gel transition occurs within the molecular weight range. This sol-gel makes the mPEG-PCL appropriate to load and deliver the drug to the inflamed area. Next, its binding affinity is increased to the colon epithelium by conjugating flagellin-derived peptide to the mPEG-PCL, which binds to TLR5 (Toll-like receptor 5) of colon epithelium. When loaded to the peptide-conjugated hydrogel, dug is released in a controllable fashion depending on the concentration of mPEG-PCL. Also, the hydrogel shows the binding specificity to intestinal cells in vitro. The results indicate several advantages of the peptide-conjugated mPEG-PCL as a drug delivery means: First, the sol-gel transition of hydrogel serves as a minimally invasive means of vehicle injection, an on-site depot of drug, and a concentration-dependent platform for controlled drug release. Second, the conjugation of flagellin-derived peptide enables drug targeting to inflamed areas when applied to the intestine, thereby reducing the drug amount compared to systemic delivery means such as oral intake or intraperitoneal injection. Lastly, the nano-scale micelle property facilitates not only drug delivery to inflamed areas but also drug invasion into the intestinal wall underneath epithelium. In conclusion, further optimization and examination of these functional advantages would enable a promising potential to address the unmet need by serving as a tunable platform for user-friendly, disease area -specific drug delivery to the intestine.

Key words: sol-gel transition, intestinal wall adhesion, inflammatory bowel disease, peptide conjugated hydrogel, flagellin derived peptide

Intestinal wall-adhesive hydrogel to study therapeutic treatment of inflammatory bowel disease

Tae Young Kim

Department of Medical Science

The Graduate School, Yonsei University

(Directed by Professor Hak-Joon Sung)

I. INTRODUCTION

Inflammatory bowel disease (IBD) is chronic inflammation of the gastrointestinal (GI) tract that may manifest as either Crohn's disease (CD) or Ulcerative colitis (UC).[1] IBD is one relapsing and lifelong disease that affects millions of patients worldwide and the global IBD treatment market is expected to reach 9,500M USD (~11 trillion won) in 2020. Patients with IBD have uncomfortable symptoms such as abdominal pain, persistent diarrhea, bloody stool, rectal bleeding, weight loss and fatigue.[2] Although the exact etiology of IBD remains unclear, we have long recognized the close relationship between IBD and such factors as environment, genetics, and diet.[3] And one of the highest possible causes is an immune system malfunction such as polarization of intestinal

immune cells toward a Th1(T helper) response.[4] IBD progression is often accompanied by an increase in granulomas and active monocytes, which produce significant amounts of eicosanoids and cytokines.[5]

Currently, depending on the severity of the disease, symptomatic treatment is being carried out, starting with anti-inflammatory drugs which include corticosteroids Dexamethasone and aminosalicylates[6], such as mesalamine[7] (Asacol HD, Delzicol, others), balsalazide (Colazal) and olsalazine (Dipentum)[8]. For those who are in the second stage, immunosuppressants such as azathioprine[9] (Azasan, Imuran), mercaptopurine[10] (Purinethol, Purixan) and methotrexate[11] (Trexall) are used. These drugs work in a variety of ways to suppress the immune response that releases inflammation-inducing chemicals into the body. Finally, in very severe cases, surgical resection is performed. However, anti-inflammatory drugs and immunosuppressants are accompanied by many side effects which are vomiting, burping, chest pain and shortness of breath through mainly non-specific oral administration [12] Side effects like these are due to absorption of drug into non-imflamed area since target-specific treatment is incapable. To overcome these side effects, target-specific drug delivery is required.

Target-specific drug delivery[13] is important to improve therapeutic efficacy and efficiency for the following reasons: 1) Drug administration protocols may be simplified. 2)Toxicity is reduced by delivering a drug to its target site, thereby reducing harmful systemic effects. 3) Drug can be administrated in a smaller dose to produce the desire effect. 4) Drug can avoid hepatic first-pass metabolism. 5) Absorption of target molecules

such as peptides and particulates is enhanced. 6) Dose is less compared to conventional drug delivery system.

For the target-specific drug delivery, we were interested in hydrogels that are widely used in the pharmaceutical field. Since the first report on the medical use of poly(2-hydroxyethyl methacrylate) hydrogels[14], research on hydrogels has continued for the past decades. Hydrogels can be classified according to various characteristics: their origin (natural, synthetic, or a combination of both), their properties (mechanical or physical), the nature of their polymer side groups (ionic or non-ionic), the type of cross-link (chemical or physical), and their response to various chemical and physical stimuli. **(Fig. 1-A)** Hydrogels can contain a considerable amount of water in a three-dimensional network.[15] As proved at successful applications in the peritoneum and various parts of the body, hydrogel has high biocompatibility due to its high water content and physicochemical similarity with the extracellular matrix[16]. In particular, the injection-type hydrogel[17] is a formulation based on a minimally invasive technique that can be crosslinked at the same time as in vivo injection and can be simply implanted into the body without a separate surgical operation. With these reasons, hydrogel is selected for the drug delivery system. We studied pathophysiology of IBD since we tried to produce the drug delivery system that can be applied to the IBD patients.

Looking at the physiological environment of IBD, the disease causes changes in the tissue environment in which the expression level of TLR5 (Toll-like receptor 5) of intestinal epithelial cells is increased. The TLR5 recognizes the bacterial locomotion

component flagellin for detecting whether bacteria have crossed the gut epithelia[18]. TLR5 responds to a monomeric form of flagellin from β- and γ-proteobacteria that constitutes the whip-like flagellar filament responsible for locomotion. Flagellin binding to TLR5 induces MyD88-dependent signaling and activates the proinflammatory transcription factor, NF-κB, in epithelial cells, monocytes, and dendritic cells, which results in activation of innate immune responses against flagellated bacteria[19]. A comparative structural analysis of the flagellin-TLR5 complexes suggests that the LRR9 loop of TLR5 centered in interface-B plays a critical role in flagellin binding[20]. Among the several residues, flagellin R89, E114, L93, and I111 cluster together in the center of interface-B. We applied the binding between TLR5 and flagellin to the specific drug delivery system for IBD patients.

Among several hydrogel candidates, we selected methoxy poly (ethylene glycol)-block-poly(ε-caprolactone) (mPEG-PCL)[21] as the basic matrix. Because of the four reasons, 1) It exists in a solution state at room temperature (25 ^{O}C). Relatively short time (1-2 mins) is required for the gelation at body temperature (37 ^{O}C), which increases tissue adhesion 2) Because gelation proceeds by simple precipitation rather than chemical crosslinking, it does not change the tissue environment. 3) mPEG-PCL consists of hydrophilic (mPEG) and hydrophobic (PCL). These amphiphilic properties give loading ability of all kinds of drugs, including both hydrophobic and hydrophilic. 4) Lastly, mPEG-PCL is easily functionalized because of the hydroxy group end of the PCL block. However, there is evident limitation of specific delivery of hydrogel to the pathogen site.

As previously reported, TLR5 physically bonds to the flagellin of bacteria. a flagellin-derived peptide was attached to the hydrogel to increase the adhesion to the inflamed area. For more specific targeting, we try to develop injectable drug delivery hydrogel system. **(Fig. 1 – B and C)**

Here, we proved the adhesion and drug delivery ability of the flagellin derived peptide conjugated hydrogel as a drug delivery system through a series of in vitro epithelial cell adhesive study and drug release test using modified trans-well method. This drug delivery platform suggests the possibility of expansion to the other diseases as well as patients with inflammatory bowel disease.

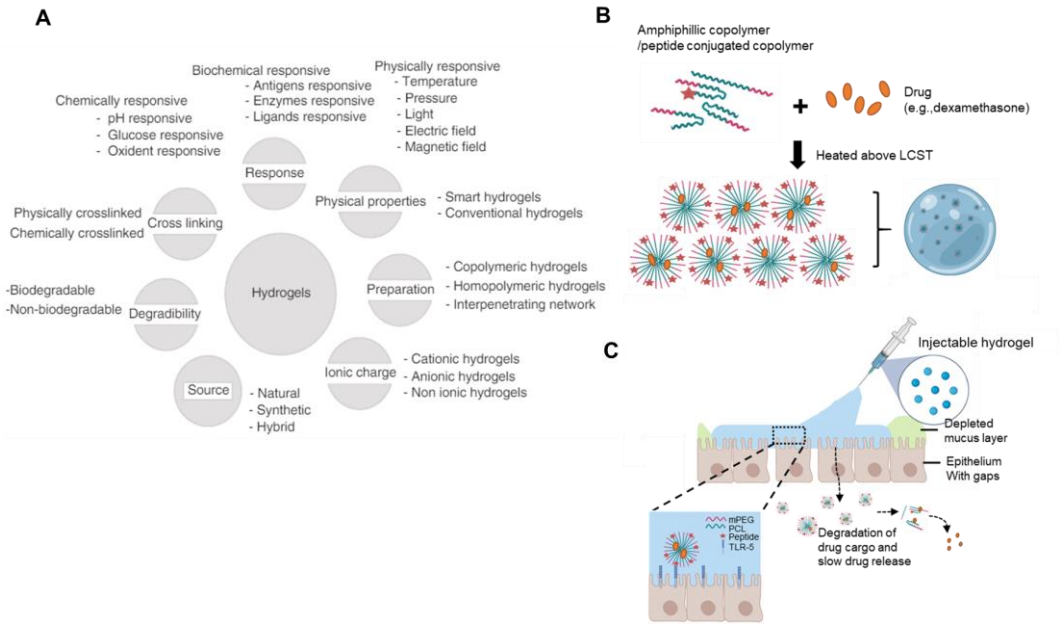

Figure 1. Hydrogels classification and schematic illustration of injectable hydrogel (A) hydrogels can be classified according to various characteristics: their origin, properities, their nature of polymer side groups, the type of cross-link, and their response to various chemical and physical stimuli. (B) A lipophilic drug is loaded into hydrogel during gelation. The drug integrates into the hydrophobic core. Amphiphillic copolymer and peptide conjugated copolymers are suspended in phosphate-buffered saline (PBS) to yield a nano-size micelle particle of various sizes. (C) Injectable hydrogel to the inflamed mucosa are presented. The inflamed mucosa is characterized by mucus depletion, accumulation of hydrogel, and increased permeability of the epithelial cell layer. Peptide conjugated hydrogels adhere to the TLR5 expressed epithelium.

II. MATERIALS AND METHODS

1. mPEG-PCL and peptide conjugated mPEG-PCL synthesis

Thermosensitive mPEG-PCL polymers were synthesized by one-step ring-opening polymerization (ROP) of caprolactone. Firstly, 7.5 g (10 mmol) of mPEG was weighed and prepared in three-neck round flask equipped with a stirring bar. Distilled 24.2 ml (22 mmol) CL was then added to the flask under vacuum conditions to remove any moisture, and the flask was submerged in an oil bath at 130 ^{O}C. Next, mPEG and CL were reacted under nitrogen purging for 1.5 hours. The synthesized polymer was then dissolved in dichloromethane, precipitated in cold diethylether, and dired overnight under vacuum condition. The mPEG-PCL diblock copolymer was prepared through ring-opening polymerization of e-CL (42 mmol) using MPEG (2 mmol) as an initiator in the presence of stannous octoate[$Sn(Oct)_2$] in diethyl ether (4 mmol), as reported previously.[22-25] peptide was coupled to the mPEG-PCL copolymer via a CDI-mediated amidation reaction as follows. (i) The hydroxyl group of mPEG-PCL (0.0130 mmol) was substituted with an imidazole leaving group via the SN2 reaction of CDI (0.0156 mmol) in dimethyl sulfoxide (DMSO; 10 mL) for 24 hours, forming imidazole-carbamated MP. (ii) ED (0.0156 mmol) was conjugated to the imidazole-carbamated mPEG-PCL through imidazole displacement via an SN2 reaction in DMSO (10 mL) for an additional 24 hours. The reactant (aminated MP) was purified using a dialysis tube (cut-off: 1~2 kDa) for three days. The obtained solution was lyophilized at -90 ^{O}C for 7 days and stored in a freezer (-20 ^{O}C) before use. (iii) peptides were conjugated to aminated mPEG-PCL in a

co-solvent of DMSO/distilled water (10 mL; 1:1 v/ v%) using DMT-MM as a coupling agent. Purification and lyophilization were carried out in the same manner as for the aminated mPEG-PCL preparation.[26-30]

2. Material characterization

The structure and molar ratio of mPEG-PCL was determined using ^{1}H-NMR ($CDCl_3$ with 0.03 % v/v TMS) spectroscopy (Avance III 400-MHz NMR spectrometer; Bruker Biospin, Billerica, MA). PCL peaks appeared at δ = 4.10 [m, $–OCH_2$], 2.41 [m, $–CH_2$], 1.74 [m, $–CH_2$], and 1.45 [m, $–CH_2$], while mPEG peaks were observed at δ = 4.13 [s, $=CH_2$], 3.28 [s, $=CH_2$] and peak related to peptide were observed at δ = 1.70 [m, $–CH_2$] of arginine. The proportions of PCL and mPEG were determined by the area ratio between the ^{1}H-NMR absorption peaks of PCL and mPEG.[31] The molecular weight and polydispersity index were determined by gel permeation chromatography (Agilent 1200 series; Agilent Technologies, Santa Clara, CA) against polystyrene standards with a PLgel 5-μm Mixed-D column (300 mm, Φ = 7.5 mm) in tetrahydrofuran at a flow rate of 1 ml min^{-1}.

3. Micelle size and Material properties (Rheometer)

The mean diameter and polydispersity (PDI) of the micelles formed in the hydrogel

precursor solutions were characterized using dynamic light scattering (DLS) (ELS-1000ZS, Otsuka Electronics Ltd., Japan). A specific concentration of solution (1 mg/mL) was added to a cuvette (HRA-271220; Ratiolab1, Am Siebenstein, Germany) and measured at 25 ^{O}C for three cycles. The hydrogel formation of the solutions was examined at 37 ^{O}C using the tilting method with glass vials containing each solution. Sol to gel transition was measured using a rheometer (Bohlin Advanced Rheometer with a parallel 20 mm plate, Malvern Instruments, UK) at temperatures ranging from 10 ^{O}C to 60 ^{O}C.[32]

4. SEM and TEM measurements of hydrogel

To monitor the morphological changes that occur as the system passes through the phase transition, samples of the 10 wt% mPEG-PCL were prepared in gel states. The hydrogel samples were then carefully transferred onto a metal stub and then quickly immersed in a liquid nitrogen bath to minimize the formation or reinforcing of the certain interaction between diblock copolymers, after which they were freeze-dried at –75 ^{O}C using a freeze dryer. Once completely dry, the diblock copolymer samples on metal stubs were coated with a thin layer of platinum using a plasma-sputtering apparatus (Emitech, K575, Japan) under an argon atmosphere. Scanning electron microscopy (SEM) (MERLIN, Zeiss, Oberkochen, Baden-Württemberg, Germany) measurements were carried out on the

platinum-coated samples.[33] The morphology of prepared micelles was observed under a transmission electron microscope (TEM) (H-6009IV, Hitachi, Japan): micelles were diluted with distilled water and placed on a copper grid covered with nitrocellulose.[34] The samples were negatively stained with phosphotungstic acid and dried at room temperature.

5. Drug release with modified trans-well method

Dexamethasone (Dex) was loaded on the inside of the 6,8,10 wt % of mPEG-PCL hydrogel to induce gradual occlusion of the hydrogel. Analysis of the volume of Dex released[35,36] by the hydrogel was performed using an Agilent Technologies 1260 Infinity II system (Agilent Technologies Inc., Santa Clara, CA) equipped with a degasser, a quaternary pump, an autosampler, and a UV detector. The samples were separated using an Agilent Poroshell, 120 EC-C18 4 μm, 46 x 100 mm (Agilent, part no. 695970-902 (T)), which was maintained at 22 ^{O}C with a detection wavelength of 242 nm. Acetonitrile-water 25-75 (v/v %) was used for the mobile phase at a flow rate of 1ml min^{-1}, and a sample injection volume of 5μL. The peaks were identified by their retention times in comparison to the external Dex calibration. 5% of Tween 80 solution in Distilled water (DW) was used as a solvent for testing the release of Dex, and the volume of Dex was measured in time intervals (1,4,7, 12, 24, 48, 72 and 96 hours).

6. Cell culture

The IEC18 cell line was obtained from the Seoul National University Hospital Cell Line Bank (Seoul, Republic of Korea). Cells were treated with 4mM Butyrate or vehicle for 24 h for gamma count analysis and flow cytometry. Cytochalasin B (2.5 μM, Sigma-Aldrich), a GLUT inhibitor, or phlorizin (100 μM, Sigma-Aldrich), an SGLT inhibitor, was administered 30 min before incubation with FDG.

7. Cytotoxicity of mPEG-PCL Micelles

The cytotoxicity of mPEG-PCL micelle was evaluated by cell viability assay on L929 cell line and IEC-18 cell line. Briefly, L929 and IEC-18 cells were plated at a density of 5×10^3 cells per well in 100 μL DMEM medium in 96-well plates and grown for 24 h. The cells were then exposed to a series of mPEG-PCL micelles at different concentrations for 48 h, and the viability of cells was measured using the CCK-8 method.

8. PCR and qPCR

Total RNA was extracted from cells and tissues by Trizol (Invitrogen) following the manufacturer's instructions and quantified using a NanoDrop™ 2000 Spectrophotometer (Thermo Fisher Scientific). Complementary DNA (cDNA) was produced by

AccuPower® CycleScript RT Premix (Bioneer) according to the manufacturer's instructions using the T-100 Thermal Cycler (Bio-Rad) and subjected to PCR on the T100 Thermal Cycler (Bio-Rad) with a primer set and a HiPi Plus 5×PCR premix (Elpisbio), followed by agarose gel electrophoresis. qPCR was carried out using cDNA, primer set, and SYBR Green PCR mix (Applied Biosystem) on StepOne Plus Real Time PCR System (Applied Biosystems), followed by melting curve analysis. Each result was normalized to the corresponding amount of glyceraldehyde 3-phosphate dehydrogenase (GAPDH) or ribosomal protein S18 (RPS18). The values were analyzed by the comparative Ct ($2^{-\Delta\Delta Ct}$) method, and further normalized to that of negative control. The primer sequences used in the reaction are listed in **Table 1**. Microarray was performed to profile the microRNA content of the TMNV using GeneChip 4.0 microRNA Microarray (Affymetrix, Japan) according to the manufacturer's instructions.

9. Western blotting

Total proteins were extracted by lysing samples with RIPA buffer (Sigma-Aldrich), followed by amount quantification using Bradford assay (Sigma-Aldrich). Protein extracts were run on a 10% (w/v) SDS–polyacrylamide gel (SDS–PAGE gel) and electro-transferred onto a nitrocellulose membrane, followed by blocking in TBST (20 mM Tris, 0.9% NaCl, 0.1% Tween 20, pH 7.4) with 5% (w/v) skin milk for 1h at RT. Membranes were incubated with primary rabbit anti-CD31 (PECAM1) (1/200, Abcam),

rabbit anti-caspase3(1/1000, Abcam), rabbit anti-Ki67(1/1000, Abcam), rabbit anti-Notch1(1/1000, Abcam) and mouse anti-β-actin(1/1000, Abcam) antibodies diluted in 5% skin milk, followed by treatment of secondary goat anti-Rabbit IgG (H+L)-HRP conjugated (1/5000, Abcam) antibodies. The signals were visualized using the Clarity Western ECL Substrate (BIORAD, Republic of Korea) according to the manufacturer's instruction, and analyzed using LAS-3000 (Fujifilm, Japan).

10. Immunofluorescence staining

Immunofluorescence staining was performed by recycling the cell plate by removing the antigen via heating with citrate buffer treatment (C9999, Sigma-Aldrich, St. Louis, MO, USA). The plate were permeabilized with 0.3 % Triton X-100 (93443, Sigma-Aldrich, St. Louis, MO, USA) in PBS for 15 min and blocked with 5 % BSA for 1 hours. The sample plate were then incubated with primary mouse anti-TLR5 (1:100 dilution; ab24590, Abcam, Cambridge, Cambridgeshire, UK), washed with PBS containing 0.5 % Tween 20, and reacted with secondary anti-rabbit conjugated to Alexa Fluor 594 (1:200 dilution; 115-545-144, Jackson ImmunoResearch Laboratories, West Grove, PA, USA) The cell nuclei were counter-stained with NucBlueTM Live ReadyProbesTM Reagents (7817, Invitrogen, Waltham, MA). Finally, the plates were subjected to optical or confocal imaging (LSM700, Zeiss, Oberkochen, Land Baden-Württemberg, Germany), followed by image analysis using ImageJ/Fifi software (NIH).

11. Statistical analysis

All the results were presented as mean ± standard deviations (SD). Statistical analysis was conducted using a t-test for more than two groups with one factor or two-way ANOVA with Bonferroni's and Tukey's post hoc analysis for more than two groups with more than one factor (SPSS 15.0; SPSS Inc.). P values are denoted in each figure and legend.

Table 1. PCR primer list

	Accession number	Primer sequence (5'-3')
TLR5	NM_002467.5	F- AAA AGC AGC AGT ATT TGA GG R- ACT AGG AAA CCG TCC TTA TG
GAPDH	NM_004235.5	F- CTC ATG ACC ACA GTC CAT GC R- TTC AGC TCT GGG ATG ACC TT
beta-Actin	NM_006500.2	F- AGC CAT GTA CGT AGC CAT CC R- CTC TCA GCT GTG GTG GTG AA
NF-kB	NM_002507.3	F- TAC CCT CAG AGG CCA GAA GA R- TCC TCT CTG TTT CGG TTG CT
MyoD88	NM_022551.2	F- GCT GAC TTG GAG CCT GAT TC R- GAT AGG CAT GTC AGG GGA GA
IL6	NM_001135.3	F- CCG GAG AGG AGA CTT CAC AG R- ACA GTG CAT CAT CGC TGT TC
IL-8(h)	NM_000346.4	F- ATG ACT TCC AAG CTG GCC GTG R- TGA ATT CTC AGC CCT CTT CAA AAA CTT

III. RESULTS

1. Synthesis and characterization of mPEG-PCL copolymer.

mPEG-PCL(MP) di-block copolymers synthesize was illustrated in **(Fig. 2-A)** by one-step ring-opening polymerization (ROP) of caprolactone. The synthesis method is comparable to previously developed PLGA-g-PEG[37], with the difference being that the monomers of lactide and glycolide were replaced by caprolactone. The molecular weight is a critical factor of MP sol-gel transition. The molecular weight of synthesized MP is affected by the amount of catalyst, temperature, reaction time, and the ratio of mPEG and PCL. We performed the experiment by adjusting the ratio of mPEG : PCL while other factors are fixed. We proceeded with the synthesis by gradually increasing the ratio of CL starting with the 1 : 5 ratio of mPEG : PCL. In the case of mPEG : PCL at a molar ratio of 1 : 5, the yield was low. At a ratio of 1 : 10, We obtained a molecular weight of 3,027 g/mol, slightly lower than the target molecular weight which is 3,200-3,500 g/mol. Finally, when the ratio of mPEG : PCL became 1 : 12.5. the target molecular weight range of 3,461 g/mol was obtained. When the ratio was increased to 1:25, the molecular weight of 8.539 g/mol waws obtained. **(Fig. 2-B)** With this results, nearly linear curve (R^2=0.9987) representing the molecular weight depending on ratio of CL to $Sn(Oct)_2$ was obtained. **(Fig. 2-C)**

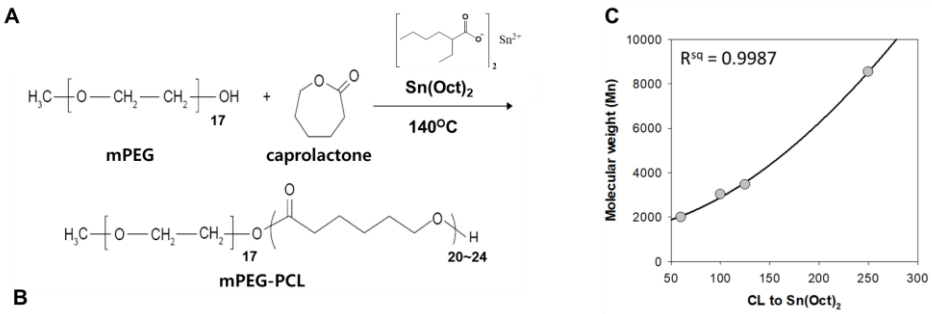

mPEG	CL	$Sn(Oct)_2$	mPEG to $Sn(Oct)_2$	$Sn(Oct)_2$ to CL	Temp. (°C)	Time (h)	Mn	Mw	PD	CL unit	mPEG%
0.01	0.05	0.001	10:1	1:50	140	1	Low				
0.01	0.1	0.001	10:1	1:100	140	1	3027	3450	1.14	20	24.8
0.01	0.125	0.001	10:1	1:125	140	1	3461	4090	1.18	24	21.7
0.01	0.25	0.001	10:1	1:250	140	1	8539	10945	1.28	68	8.8

Figure 2. Synthesis and characterization of MP di-block copolymer. (A) MP polymers synthesize was illustrated by one-step ring-opening polymerization (ROP) of caprolactone (B) The synthesis conditions and results of MP di-block copolymers are presented in the table. (C) The graph of molecular weight depending on CL to $Sn(Oct)_2$.

2. Candidate peptides screening and selection with computational binding affinity.

In order to increase the accuracy delivery of hydrogel to the inflamed region, a peptide that can physically adhere to the TLR5 expressed intestinal epithelial cells was screened using previously reported study and glide program. One receptor (TLR5) in the dataset is docked with 7 peptides contained in the dataset. **(Fig. 3-A)** Then, the 7 target peptides were ranked based on the docking score. **(Fig. 3-B)** Two peptide ,Candidate 2(QRMRELTV) and 3(QRMRELRVQ), were selected according to the docking score close to -10.[38] And also, candidate1(QRE), which includes only hot spot of flagellin amino acid, Glutamine (Gln), Arginine (Arg) and Glutamate (Glu), found in the previous study, was selected**. (Fig. 3-C)**[39] To evaluate actual adhesion to the TLR5 in vitro, fluorescamine and alpha imager assay[40] was employed. To confirm the adhesion of the three candidate peptide groups, the test was performed to the IEC-18 (Intestinal epithelial cells-18) with or without TLR5 overexpression. Candidate 1(QRE) showed the lowest IEC-18 adhesion in the TLR5 overexpressed group. On the other hand, Candidate 2(QRMRELTV) and Candidate3(QRMRELRVQ) showed high adhesion in the TLR5 overexpressed group. Compared to Candidate 1(QRE), Candidate 2 (QRMRELTV) showed increase of 43 ± 3.5 % in adhesion, and Candidate 3(QRMRELRVQ) showed an increase of 21 ± 4.12 %. Among the peptide candidates , the highest adhesion **(Fig. 3-D)** was observed in the Candidate 2 composed of 8 amino acids (QRMRELTV).[41] This correlated with computational binding affinity as studied by glide program.

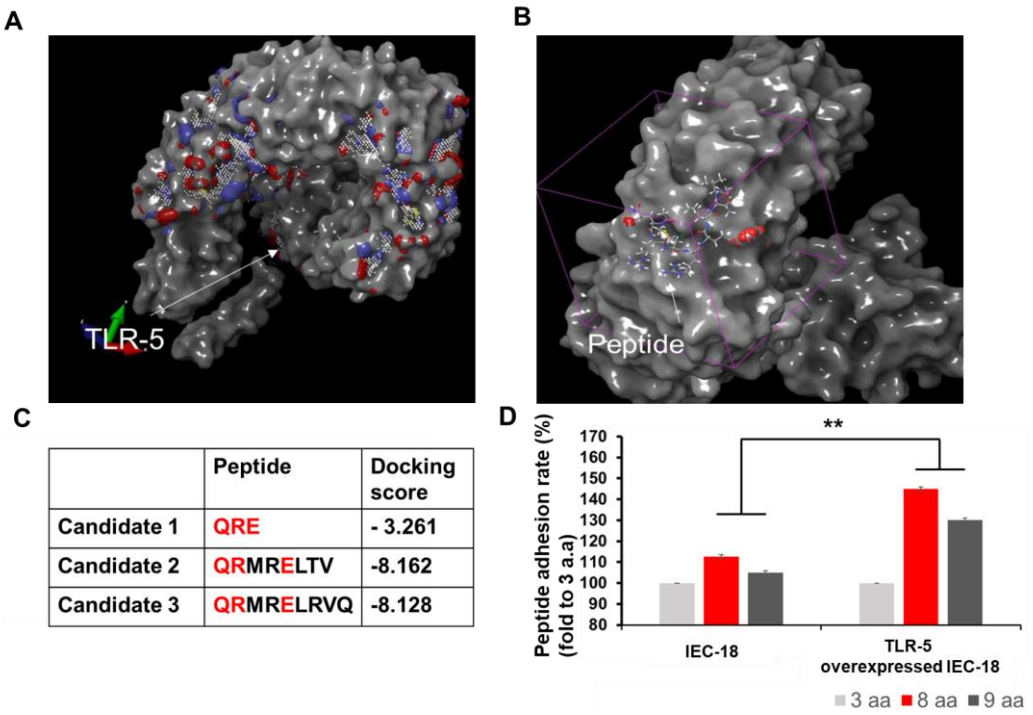

	Peptide	Docking score
Candidate 1	QRE	- 3.261
Candidate 2	QRMRELTV	-8.162
Candidate 3	QRMRELRVQ	-8.128

Figure 3. Binding interface and ranking the scores of flagellin derived peptide candidates. (A-B) Illustration of the multiple grid arrangement method. Red dots on the protein indicate a predicted peptide binding site, and blue dots show receptor grids for peptide docking. The multiple grid arrangement method can cover an entire space of any predicted ligand-binding site automatically. (C) The complex models were arranged according to their scores, and rankings were assigned. Selected peptide candidates are listed in the table. (D) In vitro adhesion test of peptide candidates to the IEC-18 (Intestinal epithelial cells-18) with or without TLR5 overexpression. All data are shown as the mean ± S.D. *$p < 0.05$, **$p < 0.01$, and ***$p < 0.001$ between lined groups.

3. Preparation and 1H NMR characterization of peptide conjugated MP

A scheme for conjugation of peptides to the MP backbone is shown. **(Fig. 4-A)** Conjugation of peptide to MP was confirmed with ^{1}H NMR analysis using a solvent of chloroform-d_6. [31] The signals at 3.53 and 3.68 ppm were assigned to the methyl and methylene groups of mPEG, respectively. The peaks (yellow circle) at 4.21–4.39, 3.73, 2.09–2.12, and 1.88–1.97 ppm were attributed to PCL. Three peaks related to peptide (red circle) were observed at 3.40 ppm for the aspartic acid, at 4.08 ppm for the of glycine, and at 1.70 ppm for the arginine. The relative intensities of the signals at 3.53 and 3.40 ppm, which were assigned to the methyl group of mPEG (brown circle). **(Fig. 4-B)** To quantify the actual amount of peptide in the peptide conjugated polymers, Sakaguchi assay which detects the guanidine group in the arginine of peptide the was employed.[40] MP-Peptide $_{1.0, 2.0, 3.0, 4.0}$ represents how much peptide should be theoretically conjugated when 1.0, 2.0, 3.0, 4.0 mM of peptide are reacted with MP. The UV–Vis spectra of the MP and MP-peptide samples treated with Sakaguchi reagents. The MP-peptide samples exhibited maximum absorption around 520 nm and we could observe normalized absorbance of approximately 0.1, 0.17, 0.25, 0.31 from MP-Peptide $_{1.0, 2.0, 3.0, 4.0}$ respectively**. (Fig. 4-C)** With this normalized absorbance, the peptide concentration calculated using the standard curve of acetylated glycine which content is fixed. **(Fig. 4-D)** In the case of MP-peptide$_{4.0}$, 3.1 ± 0.22mM of peptide was attached to the MP implying that approximately 70% of the peptide was stably attached to the MP. In the case of MP-peptide$_{1.0, 2.0,3.0,}$ 0.8 ± 0.41mM, 1.6 ± 0.4mM, 2.7 ± 0.11mM of peptide was respectively attached to the MP with conjugation

percentage of 70- 75%. From the results above, we confirmed that the peptide conjugated MP can be stably synthesized.

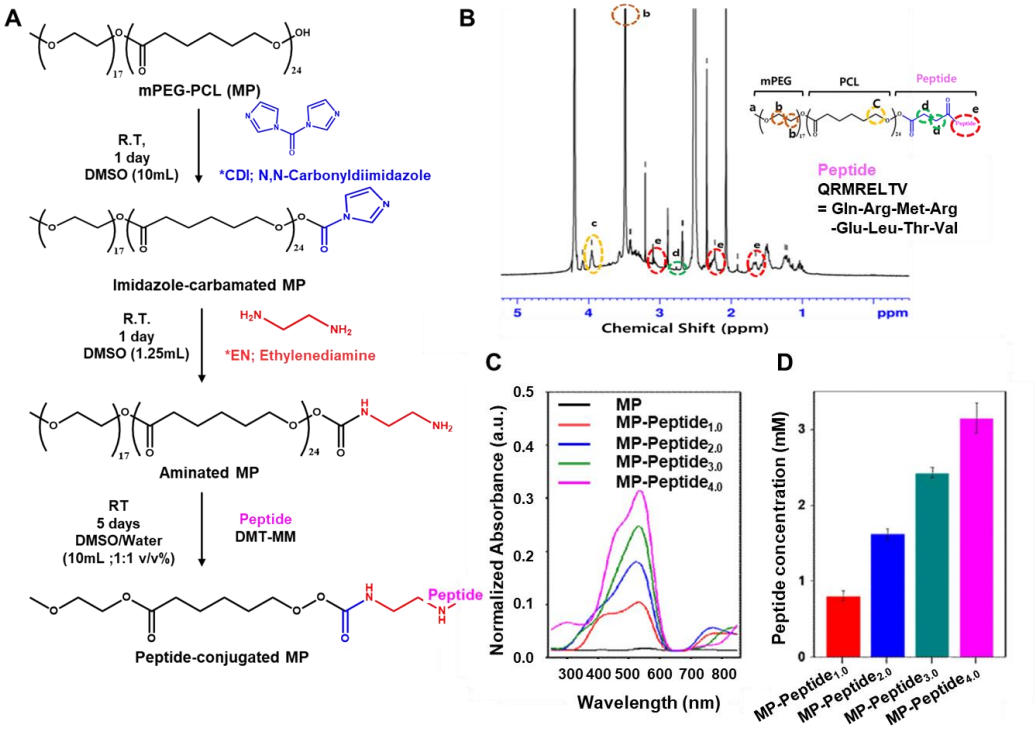

Figure 4. Schematic illustration and 1H NMR spectra of peptide-conjugated MP. (A) The hydroxyl group at the one side of mPEG-PCL was aminated with ED via the imidazole displacement of SN2 reaction using CDI, followed by conjugation of peptide via condensation reaction using DMT-MM as a condensing agent. CDI-N,N-carbonyldiimidazole; ED-ethylenediamine. (B) 1H NMR spectra of peptide conjugated hydrogel measured in a solvent of chloroform-d_6. (C-D) Sakaguchi assay was analyzed for confirmation of peptide contents. Abbreviations: MP, mPEG-PCL

4. Rheological properties of hydrogel.

We demonstrated the sol-gel transition by precipitation of MP-peptide mixed copolymer. The copolymer exists as a solution at room temperature (25 ^{O}C) and becomes a gel around the body temperature (37 ^{O}C) which means its suitability as a drug delivery system. **(Fig. 5-A)** The viscoelasticity of 5, 10 (w/v) % hydrogel was measured through a frequency sweep of a rheometer, a powerful theology tools for the study of fluid and soft body systems. **(Fig. 5-B)**

Compared to the sol state, the storage modulus(G') in the gel state showed a larger increase than the loss modulus(G"). In the body temperature range (=37 ^{O}C), the storage modulus (G') was greater than the loss modulus (G") in both 5 (w/v) % and 10 (w/v) % hydrogel. It implies that the hydrogel exists as gel state at body temperature. The elastic modulus and elasticity of the hydrogel were calculated by the storage(G') and loss modulus(G") of hydrogels (5,10 (w/v) %) measured through frequency sweep. A stiffer material, 10 (w/v) % hydrogel in **(Fig. 5-C)**, will be characterized by a 4 times higher elastic modulus than that of 5 (w/v) % hydrogel. High elastic modulus and low elasticity indicate high strength of the material. To understand the sol-gel transition process of 5 (w/v) % MP hydrogel, temperature sweep measurements were performed. More specifically, the storage modulus (G') represented the elastic behavior and the loss modulus (G") denoted the viscous behavior were monitored as a function with temperature.[35] As illustrated in **(Fig. 5-D)**, it was clearly observed that the loss modulus(G") was greater than storage modulus

(G') as temperature was lower than 32 ^{O}C, corresponding to the sol state of system. As gelation proceeds, the storage modulus(G') was equal to loss modulus(G") at 32 ^{O}C, indicating the sol–gel transition temperature of system. Subsequently, storage(G') and loss(G") increased further with increasing temperature, reaching its highest at 43 ^{O}C.

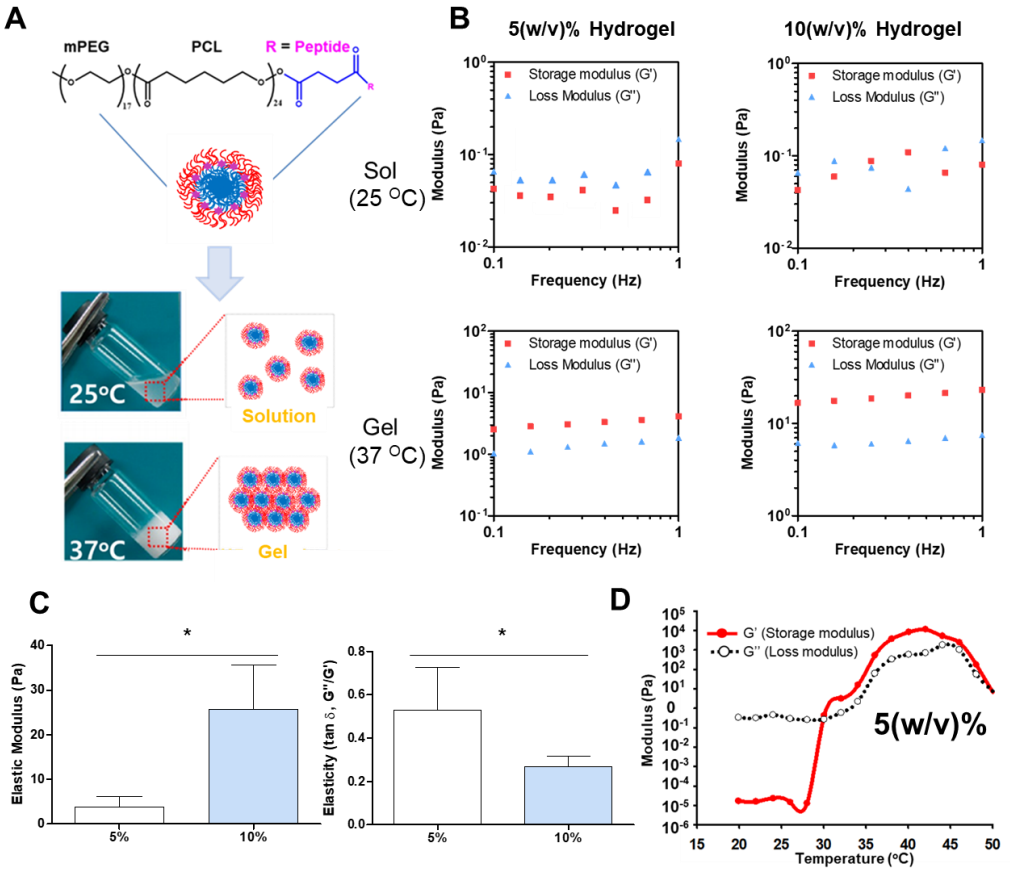

Figure 5. Sol–gel transition behavior of mPEG-PCL mechanical properties of hydrogel

(A) Thermosensitive MP micelles are prepared through self-assembly of amphiphilic di-block copolymers. (B-C) Rheological properties was detected using rheometer. (D) hydrogel sol-gel transition was observed with temperature sweep measurements. All data are shown as the mean ± S.D. *p < 0.05, **p < 0.01, and ***p < 0.001 between lined groups.

5. Size distribution of spherical micelles and in vitro drug release.

The morphology and size distribution of the MP hydrogel was measured by scanning electron microscopy (SEM), transmission electron microscope (TEM) and dynamic light scatting (DLS). To evaluate the structure of MP in aqueous solution, we prepared a sample by lyophilizing 5 (w/v) % MP hydrogel. The highly interconnected porous morphologies with macropores larger than 10 μm and irregular shapes are observed. To observe micelle structure in MP hydrogel, we prepared a sample by lyophilizing low concentration (= 10^{-2} (w/v) %) MP hydrogel. **(Fig. 6-A and B)** The particle size of MP micelles at the low concentration of MP hydrogel measured by DLS was 105 ± 5.38 nm (PDI = 0.228). **(Fig. 6-C)** Nano size micelles means, these structures penetrate in the tissue system, facilitate easy uptake of the drug by cells, permit an efficient drug delivery and ensure action at the targeted location.

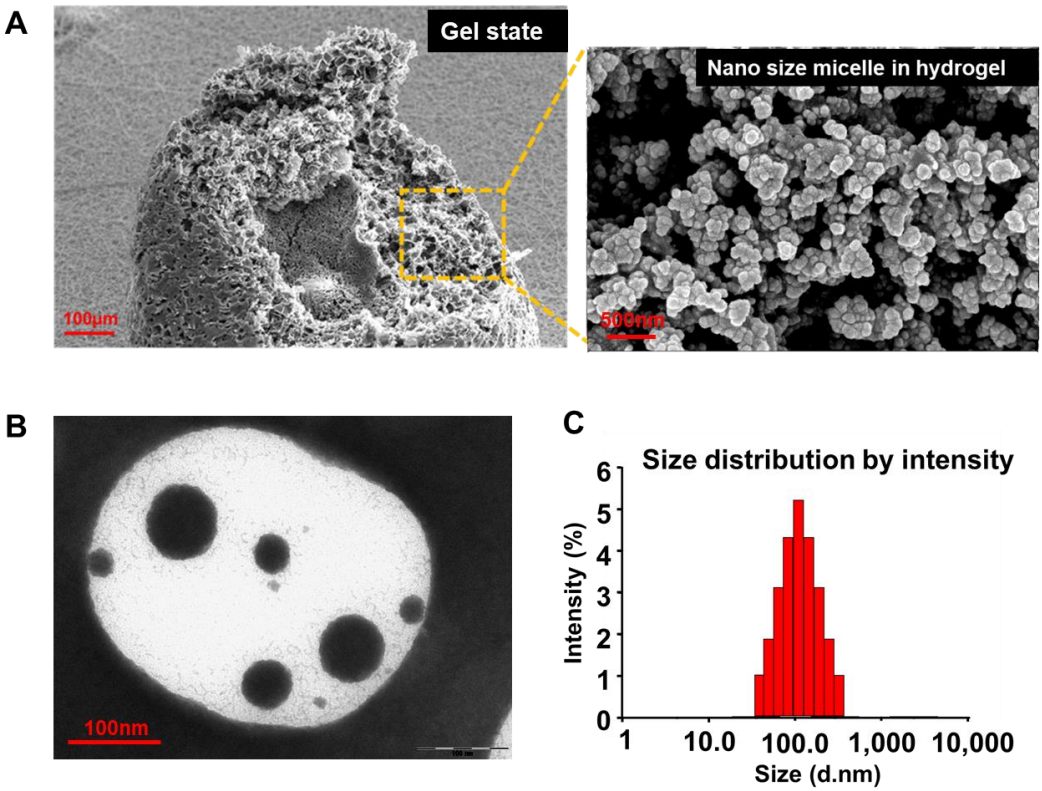

Figure 6. Structure of MP in aqueous solution and size distribution of spherical micelles. (A) The morphology of MP was observed under a SEM. And nano size micelle structure was observed under a SEM and TEM at the low concentration ($<10^{-2}$) of MP hydrogel. (C) MP basically formed spherical micelle structure in an aqueous environment and mean diameter (=105± 5.38 nm) of the spherical micelles was detected by DLS particle size distributions.

6. In vitro disease modeling and evaluation

The cytotoxicity of MP, peptide, MP-peptide on the L929, IEC-18 cells were evaluated using the Cell Counting Kit-8 (CCK-8) assay (Promega, Madison, WI) according to the manufacturer's instructions. As shows in **(Fig. 7-A)**, The cell only treated with DMEM media was selected as control group, treated with MP kept a viability of 93.3%. Cells treated with peptide still kept a viability of 95.6% even at a high concentration of 20μM peptide and MP-peptide (peptide conjugated MP) kept a viability of 92.4%. We can observe no significant cell cytotoxicity in every group.

In order to make in vitro disease model, we treat butyrate to the IEC-18. Butyrate induced TLR5 mRNA expression in a dose- and time-dependent manner with the highest levels (approximately 4 times higher than control group) of expression noted after treatment with 4 mM of butyrate for 24 hours[42] **(Fig. 7-B)**.

With TLR-5 overexpressed epithelial cells, we treated 100ng/ml flagellin as positive control and 20μM candidate peptides to observe cascade signaling of NF-kB, IL-6 and TNF-α mRNA expression with qRT-PCR.[43] **(Fig. 7-C)** The cell signaling means that it is caused by the binding of the peptide and TLR5 receptor on the epithelial cell surfaces which means peptide candidate are well attached to TLR5. Compared with control group, in the group treated with flagellin, NF-kB, IL-6, TNF- α expression level of was increased by 32.7 ± 4.72, 58.5 ± 5.12, 47.2 ± 2.98, respectably. Also, among peptide candidate, the peptide composed of 8 amino acid (QRMRELTV) NF-kB, IL-6, TNF- α expression level of mRNA was

increased by 10.2 ± 1.72, 8.75 ± 3.52, 13.8 ± 3.98, respectably. Peptide composed of 8 amino acid slightly similar cell signaling of flagellin treated group. With this result, we confirm that the peptide composed of 8 amino acid has the best TLR5 adhesion ability. This correlated with NF-kB and IL-6 expression as studied by Western blots. **(Fig. 7- D and E)**

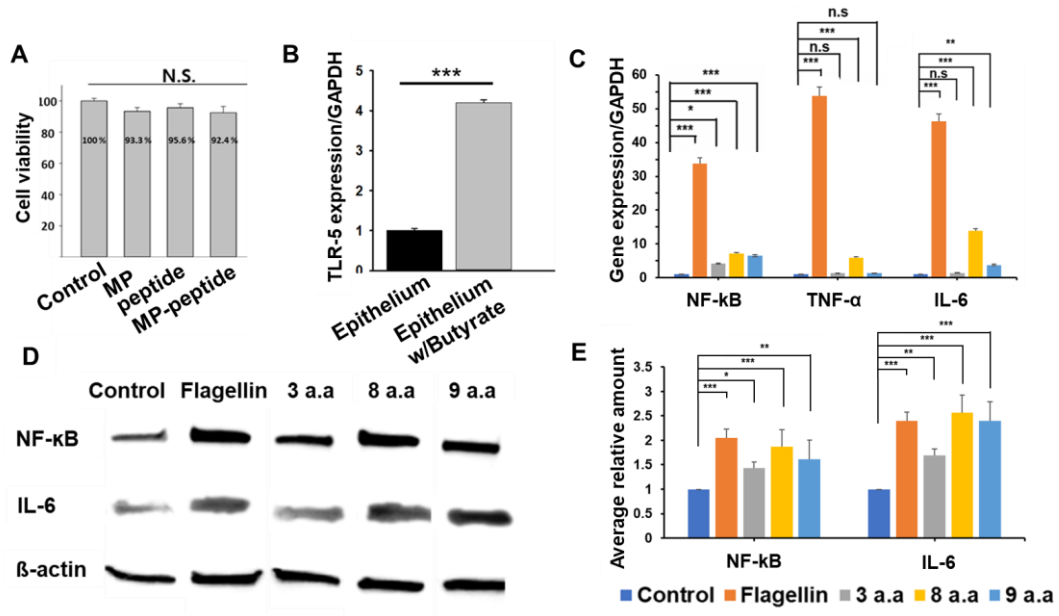

Figure 7. Cell signaling by binding of flagellin derived peptide and TLR5 receptor. (A) Biocompatibility was observed in L929 and IEC-18 cells. (B) qRT-PCR showing TLR5 mRNA expression in IEC-18 cells treated with physiological concentration of butyrate (4mM) for 24h. (C) qRT-PCR showing IL-6, TNF- α mRNA expression in TLR5 overexpressed IEC-18 cells treated with 100ng/ml flagellin and 20μM peptides (D-E) Compared with control group, the expression of nuclear protein of NF-κB, total protein of IL-6 significantly increased in flagellin (Positive control) group and slightly increased in peptide composed of 8 a.a(QRMRELTV) group. Abbreviations: a.a , amino acid. All data are shown as the mean ± S.D. *p < 0.05, **p < 0.01, and ***p < 0.001 between lined groups.

7. In vitro peptide conjugated MP adhesion of TLR5

Backbone hydrogel and MP hydrogel adhesion to the IEC-18 surfaces was confirmed in comparison with or without TLR5 overexpression. Following the pre-defined washing, the remaining peptide conjugated MP hydrogel (MP-peptide hydrogel) (red fluorescent labeled) was located between the cells, also found at cell membrane surface. In particular, the hydrogel adhesion was clearly increased to TLR5 overexpressed IEC-18. Indicating that conjugation of flagellin-derived peptide successfully promoted target specific hydrogel adhesion. **(Fig. 8-A)** This result was also confirmed by the quantitative results from image analysis of the mean intensity of hydrogel per cells. Compared normal IEC-18, 0.04 ± 0.005 of adhesive MP-peptide hydrogel intensity was confirmed from in the TLR5 overexpressed IEC-18, which was significantly higher than that in normal IEC-18 (0.02 ± 0.0048). (P <0.01). **(Fig. 8-B and C)**

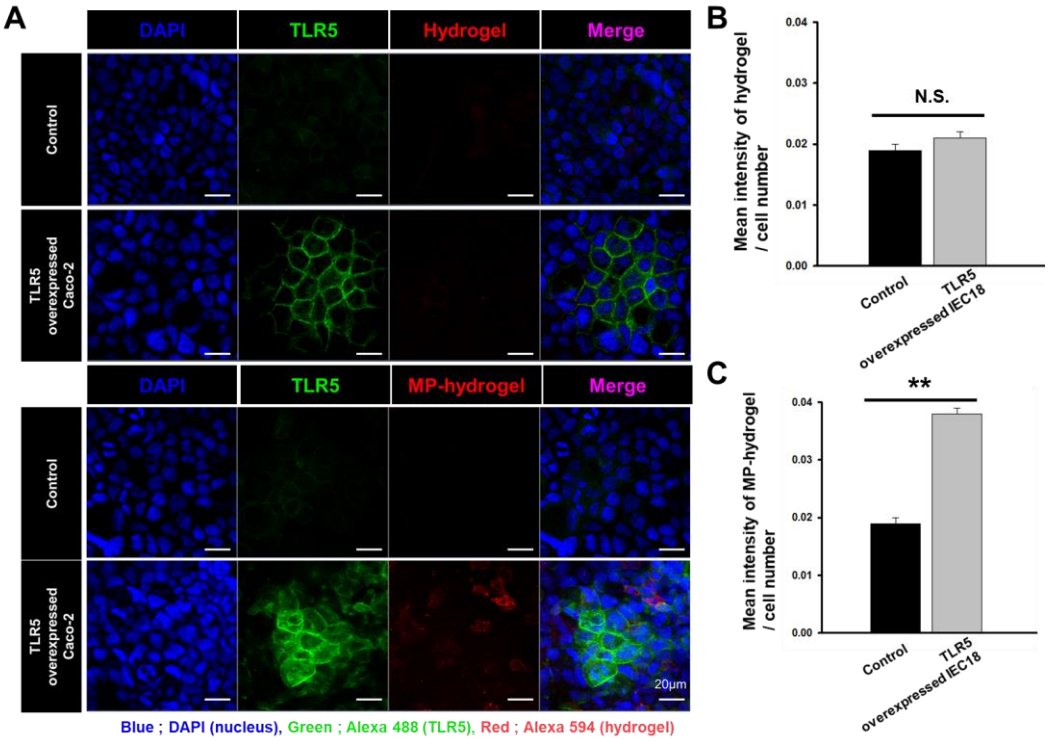

Figure 8. Peptide conjugated hydrogel attachment of TLR5 overexpressed epithelial cells. (A-C) Immunocytochemical identification of TLR5 overexpressed IEC-18 and MP-peptide hydrogel adhesion. MP-peptide was identified by alexa 594^{TM} NHS Ester Subbinimidyl Ester (red) IEC-18 by alexa 488^{TM}(green) immunostainign. The nuclei of all cells were idenrifed by DAPI(blue). All data are shown as the mean ± S.D. *p < 0.05, **p < 0.01, and ***p < 0.001 between lined groups.

8. In vitro drug release test of MP-peptide with various concentration

Among various IBD drugs, we used Dex as a model drug. In vitro release behaviors of Dexamethasone (Dex) from MP-peptide hydrogel was investigated using a modified transwell drug release method. In comparison with MP-peptide hydrogel, 10 w/v % MP-peptide hydrogel showed a much slower cumulative release behavior. As shown in **(Fig. 9-A)**, 23 ± 4.04% of Dex was released from MP-peptide hydrogel in the first 12 hours, which was significantly lower than that in 6, 8 w/v% of MP-peptide hydrogel group (37 ± 6.22% and 32 ± 4.72% respectively. P <0.01). [35,36,44] In the 48 hours, 60.6 ± 5.28% of Dex was released from MP-peptide hydrogel, which was significantly lower than that in 6, 8 w/v% of MP-peptide hydrogel group (98.7 ± 1.1% and 78.0± 3.62% respectively. P <0.001). Control of drug release depending on the concentration of MP-peptide hydrogel means high potential as a drug delivery system.

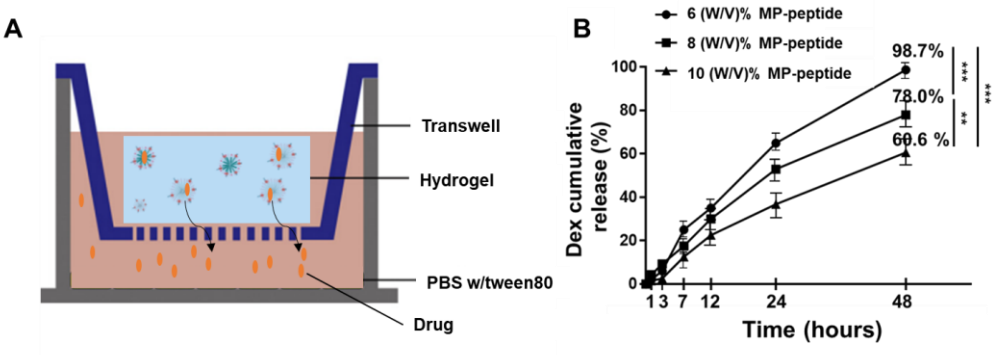

Figure 9. Drug release from various concentration of MP hydrogel. (A) Schematic illustration of modified transwell drug release test. (B) Release behavior of Dex from Dex loaded MP hydrogel was observed using HPLC. All data are shown as the mean ± S.D. *p < 0.05, **p < 0.01, and ***p < 0.001 between lined groups.

IV. DISCUSSION

Inflammatory bowel disease(IBD) is a disease that cause chronic inflammation of the gastro-intestinal tract, and has principal forms of Crohn's disease and ulcerative colitis. The therapeutic approach to patients with IBD includes three aspects, pharmacological therapy, nutritional support, and surgical intervention. Local and systemic administration of mesalazine is used in early stages, systemic corticosteroids, immune suppressive agents such as azathioprine, 6-mercaptopurine, TNA-α inhibitor are advised.

Because IBD medication such as corticosteroid, immunosuppressive agent might cause adverse side effect including an increased susceptibility to infection, medical therapy for IBD need a balance of intended therapeutic effects and unwanted adverse side effects. For achieving and/or optimizing the desired therapeutic effect and minimizing adverse effects, various drug delivery approaches that developed in decades. Because pharmacokinetic and pharmacodynamic properties of oral formulations for IBD patient drug delivery rely on pH-, time-, microflora-, or pressure-triggered mechanisms, novel disease-targeted drug delivery strategy development is an important challenge.

MP-peptide hydrogel as a drug delivery system use specific features of the inflamed region. Here, we demonstrate that MP-peptide hydrogel preferentially adhere to TLR5 expressed epithelial cell surfaces. Additionally, flagellin plays a role of pathogen in IBD pathophysiology, result in increasing level of NF-kB, IL-6, TNF-α expression level. In that peptide candidate attached to TLR5 and slightly increase the expression level of NF-kB, IL-6, and TNF-α, MP-peptide hydrogel may has a antagnostic effect to hydrogel.

The structure of MP-peptide hydrogel in aqueous solution, highly interconnected porous morphologies and irregular shapes are observed. However, in the low concentration of MP-peptide hydrogel in aqueous solution, the nano-size of the micelle are observed. These micelle structure means interconnected gel like porous morphologies consist of micelles interaction by precipitation. The nano size micelle structures of MP-peptide represent possibility of drug delivered directly to the inflamed intestine and then gradually drug release.

Potential applications are not limited to IBD but include any disease where controlled drug release at a distinct location is desired. Through attaching to the inflamed mucosa and selectively releasing drug at the site of inflammation, this system has the potential to prolong local drug availability, minimize systemic drug absorption, reduce dosing frequency, and lower the burden on the patient, all of which should improve compliance, reduce the risk for systemic toxicity, and maximize therapeutic efficacy.

This study suggests that MP-peptide hydrogel generate a reservoir of drug at the site of inflammation, thereby gradually release of local drug availability. Drug delivery using MP-peptide hydrogel direct injection to the target region may thus allow for less frequent dosing in patients with IBD. Compared with other drug delivery systems targeting the inflamed colon, peptide conjugated hydrogel has several potential advantages. First, the MP-peptide hydrogel described here is made from a nontoxic, FDA approval compound, which should facilitate rapid translation into the clinic. Second, the characteristic of being sol at room temperature and sol at body temperature is suitable for target drug delivery.

Third, a functionalized peptide to the hydrogel increase the adhesion of the inflamed area. Lastly, depending on the concentration of hydrogel, the release rate of the drug can be controlled.

V. CONCLUSION

In summary, this study offers a novel solution to a long-standing issue in specific target drug delivery by demonstrating the potent theragnostic function of peptide conjugated hydrogel. This theragnostic effect can be exerted by the synergistic function of corticoid steroid drug such as dexamethasone. Moreover, MP-peptide hydrogel was validated not only in the adhesion effect in vitro experiments but also released amount of drug is controllable depending on the concentration of MP-peptide hydrogel. And most importantly, target specific drug delivery, reducing the cost and burden to patients. These promising results suggest that peptide conjugated hydrogel is a potential drug delivery platform and therapy for IBD patients.

REFERENCES

1. Bunu D-M, Timofte C-E, Ciocoiu M, Floria M, Tarniceriu C-C, Barboi O-B, et al. Cardiovascular manifestations of inflammatory bowel disease: pathogenesis, diagnosis, and preventive strategies. Gastroenterology research and practice 2019;2019.
2. Gohil K, Carramusa B. Ulcerative colitis and Crohn's disease. Pharmacy and Therapeutics 2014;39:576.
3. Sartor RB. Mechanisms of disease: pathogenesis of Crohn's disease and ulcerative colitis. Nature clinical practice Gastroenterology & hepatology 2006;3:390-407.
4. Kidd P. Th1/Th2 balance: the hypothesis, its limitations, and implications for health and disease. Alternative medicine review 2003;8:223-46.
5. Baumgart DC, Carding SR. Inflammatory bowel disease: cause and immunobiology. The Lancet 2007;369:1627-40.
6. Marshall J, Irvine E. Rectal aminosalicylate therapy for distal ulcerative colitis: a meta-analysis. Alimentary pharmacology & therapeutics 1995;9:293-300.
7. Thomsen OØ, Cortot A, Jewell D, Wright JP, Winter T, Veloso FT, et al. A comparison of budesonide and mesalamine for active Crohn's disease. New England Journal of Medicine 1998;339:370-4.
8. Kane SV, Sumner M, Solomon D, Jenkins M. Twelve-month persistency with oral 5-aminosalicylic acid therapy for ulcerative colitis: results from a large pharmacy prescriptions database. Digestive diseases and sciences 2011;56:3463-70.
9. Candy S, Wright J, Gerber M, Adams G, Gerig M, Goodman R. A controlled double blind study of azathioprine in the management of Crohn's disease. Gut 1995;37:674-8.
10. D'Haens G, Baert F, Van Assche G, Caenepeel P, Vergauwe P, Tuynman H, et al. Early combined immunosuppression or conventional management in patients with newly diagnosed Crohn's disease: an open randomised trial. The Lancet 2008;371:660-7.
11. Thomaz MA, Acedo SC, de Oliveira CC, Pereira JA, Priolli DG, Saad MJ, et al. Methotrexate is effective in reactivated colitis and reduces inflammatory alterations in mesenteric adipose tissue during intestinal inflammation. Pharmacological research 2009;60:341-6.
12. Lankarani KB, Sivandzadeh GR, Hassanpour S. Oral manifestation in inflammatory bowel disease: a review. World journal of gastroenterology: WJG 2013;19:8571.

13. Peynshaert K, Devoldere J, De Smedt SC, Remaut K. In vitro and ex vivo models to study drug delivery barriers in the posterior segment of the eye. Advanced Drug Delivery Reviews 2018;126:44-57.
14. Peppas NA, Moynihan HJ, Lucht LM. The structure of highly crosslinked poly (2-hydroxyethyl methacrylate) hydrogels. Journal of biomedical materials research 1985;19:397-411.
15. Mansur HS, Oréfice RL, Mansur AA. Characterization of poly (vinyl alcohol)/poly (ethylene glycol) hydrogels and PVA-derived hybrids by small-angle X-ray scattering and FTIR spectroscopy. Polymer 2004;45:7193-202.
16. Dash M, Chiellini F, Ottenbrite RM, Chiellini E. Chitosan—A versatile semi-synthetic polymer in biomedical applications. Progress in polymer science 2011;36:981-1014.
17. Glogau RG, Kane MA. Effect of injection techniques on the rate of local adverse events in patients implanted with nonanimal hyaluronic acid gel dermal fillers. Dermatologic surgery 2008;34:S105-S9.
18. Yang J, Yan H. TLR5: beyond the recognition of flagellin. Cellular & molecular immunology 2017;14:1017-9.
19. Yoon S-i, Kurnasov O, Natarajan V, Hong M, Gudkov AV, Osterman AL, et al. Structural basis of TLR5-flagellin recognition and signaling. Science 2012;335:859-64.
20. Song WS, Jeon YJ, Namgung B, Hong M, Yoon S-i. A conserved TLR5 binding and activation hot spot on flagellin. Scientific reports 2017;7:1-11.
21. Lu C, Guo S, Liu L, Zhang Y, Li Z, Gu J. Aggregation behavior of MPEG-PCL diblock copolymers in aqueous solutions and morphologies of the aggregates. Journal of Polymer Science Part B: Polymer Physics 2006;44:3406-17.
22. Kim MS, Hyun H, Cho YH, Seo KS, Jang WY, Kim SK, et al. Preparation of methoxy poly (ethyleneglycol)-block-poly (caprolactone) via activated monomer mechanism and examination of micellar characterization. Polymer Bulletin 2005;55:149-56.
23. Kim MS, Hyun H, Seo KS, Cho YH, Won Lee J, Rae Lee C, et al. Preparation and characterization of MPEG–PCL diblock copolymers with thermo-responsive sol–gel–sol phase transition. Journal of Polymer Science Part A: Polymer Chemistry 2006;44:5413-23.
24. Lin G, Cosimbescu L, Karin NJ, Gutowska A, Tarasevich BJ. Injectable and thermogelling hydrogels of PCL-g-PEG: mechanisms, rheological and enzymatic degradation properties. Journal of Materials Chemistry B 2013;1:1249-55.
25. Storey RF, Sherman JW. Kinetics and mechanism of the stannous octoate-catalyzed bulk polymerization of ε-caprolactone. Macromolecules

2002;35:1504-12.
26. Kunishima M, Kawachi C, Hioki K, Terao K, Tani S. Formation of carboxamides by direct condensation of carboxylic acids and amines in alcohols using a new alcohol-and water-soluble condensing agent: DMT-MM. Tetrahedron 2001;57:1551-8.
27. Mildner R, Menzel H. Facile synthesis of pH-responsive glycopolypeptides with adjustable sugar density. Journal of Polymer Science Part A: Polymer Chemistry 2013;51:3925-31.
28. Wang B, Liu H, Wang Z, Shi S, Nan K, Xu Q, et al. A self-defensive antibacterial coating acting through the bacteria-triggered release of a hydrophobic antibiotic from layer-by-layer films. Journal of Materials Chemistry B 2017;5:1498-506.
29. Rostamizadeh K, Manafi M, Nosrati H, Manjili HK, Danafar H. Methotrexate-conjugated mPEG–PCL copolymers: a novel approach for dual triggered drug delivery. New Journal of Chemistry 2018;42:5937-45.
30. Lee YS, Kim HJ, Yang DH, Chun HJ. Preparation and anticancer activity evaluation of self-assembled paclitaxel conjugated MPEG-PCL micelles on 4T1 cells. Journal of industrial and engineering chemistry 2019;71:369-77.
31. Kim HJ, You SJ, Yang DH, Chun HJ, Kim MS. Preparation of novel RGD-conjugated thermosensitive mPEG-PCL composite hydrogels and in vitro investigation of their impacts on adhesion-dependent cellular behavior. Journal of Industrial and Engineering Chemistry 2020;84:226-35.
32. Xiong W, Peng L, Chen H, Li Q. Surface modification of MPEG-b-PCL-based nanoparticles via oxidative self-polymerization of dopamine for malignant melanoma therapy. International journal of nanomedicine 2015;10:2985.
33. Khalkhali M, Rostamizadeh K, Sadighian S, Khoeini F, Naghibi M, Hamidi M. The impact of polymer coatings on magnetite nanoparticles performance as MRI contrast agents: a comparative study. DARU Journal of Pharmaceutical Sciences 2015;23:45.
34. Chen Y, Chen X, Chen Y, Wei H, Lin S, Tian H, et al. Preparation, characterisation, and controlled release of sex pheromone-loaded MPEG-PCL diblock copolymer micelles for Spodoptera litura (Lepidoptera: Noctuidae). PloS one 2018;13:e0203062.
35. Gong CY, Dong PW, Shi S, Fu SZ, Yang JL, Guo G, et al. Thermosensitive PEG–PCL–PEG hydrogel controlled drug delivery system: sol–gel–sol transition and in vitro drug release study. Journal of pharmaceutical sciences 2009;98:3707-17.
36. Wang X, Hu H, Wang W, Lee KI, Gao C, He L, et al. Antibacterial modification of an injectable, biodegradable, non-cytotoxic block copolymer-based physical gel with body temperature-stimulated sol-gel transition and

controlled drug release. Colloids and Surfaces B: Biointerfaces 2016;143:342-51.
37. Tarasevich BJ, Gutowska A, Li XS, Jeong BM. The effect of polymer composition on the gelation behavior of PLGA-g-PEG biodegradable thermoreversible gels. Journal of Biomedical Materials Research Part A: An Official Journal of The Society for Biomaterials, The Japanese Society for Biomaterials, and The Australian Society for Biomaterials and the Korean Society for Biomaterials 2009;89:248-54.
38. Ban T, Ohue M, Akiyama Y. Multiple grid arrangement improves ligand docking with unknown binding sites: Application to the inverse docking problem. Computational biology and chemistry 2018;73:139-46.
39. Zhou Z, Liu H, Gu G, Wang G, Wu W, Zhang C, et al. Immunoproteomic to identify antigens in the intestinal mucosa of Crohn's disease patients. PLoS One 2013;8:e81662.
40. Jeong K, Chung WY, Kye YS, Kim D. ABri peptide aggregation quantification by fluorescamine and alpha imager assay. Journal of Industrial and Engineering Chemistry 2011;17:427-9.
41. Bao W, Wang Y, Fu Y, Jia X, Li J, Vangan N, et al. mTORC1 regulates flagellin-induced inflammatory response in macrophages. PLoS One 2015;10:e0125910.
42. Thakur BK, Dasgupta N, Ta A, Das S. Physiological TLR5 expression in the intestine is regulated by differential DNA binding of Sp1/Sp3 through simultaneous Sp1 dephosphorylation and Sp3 phosphorylation by two different PKC isoforms. Nucleic acids research 2016;44:5658-72.
43. Kim J, Seo M, Kim SK, Bae YS. Flagellin-induced NADPH oxidase 4 activation is involved in atherosclerosis. Scientific reports 2016;6:1-16.
44. Lee HJ, Jeong B. ROS-Sensitive Degradable PEG–PCL–PEG Micellar Thermogel. Small 2020;16:1903045.

ABSTRACT(IN KOREAN)

염증성 장 질환 치료 연구를 위한 소장벽 점착성 하이드로겔 개발

<지도교수 성 학 준>

연세대학교 대학원 의과학과

김 태 영

염증성 장 질환(IBD)는 크론병과 궤양성대장염의 한 형태로 장내 염증성 병인으로 정의된다. 근대화, 서양식 식단 등의 원인으로 인해 IBD 환자 수가 급격히 증가하고 있으며 대증적 치료수단을 이용한 증상완화에 초점을 맞추고 있다. 현재 IBD 치료약인 항염증제와 면역억제제는 구강 섭취로 소장과 대장에 전달된다. 위 약물은 설사, 혈변, 면역력 감소등의 부작용을 동반하는데 이는 염증 부위로의 표적 약물 전달이 불가능하기 때문이다. 이를 극복하기 위해 효율적인 장벽 특이적 약물전달 치료수단이 필요하다. 여기서, 우리는 mPEG-PCL를 기본 모체로 장벽 염증부위 특이적 약물 전달 하이드로겔을 개발하였다. 약물전달체의 장벽부착능력을 증가시키기 위해 편모 유래 펩타이드를 하이드로겔에 부착하였다. 편모는 장외벽에 발현하는

TLR5와 상호작용을 하는 펩타이드이다. 우리가 개발한 약물전달체는 상온에서 졸 상태로 존재하다 체온에서 젤상태가 된다. 이러한 졸 젤 전이는 약물을 담지하고 염증부위에 전달하는데 유용하다. 또한, 약물전달체의 농도를 조절함에 따라 약물의 방출 속도 조절이 가능하다. 표적 특이적 약물전달체의 개발은 몇 가지 이점을 지닌다. 첫째, 표적 특정 약물 전달을 통해 염증 부위에만 약물을 전달할 수 있다. 따라서, 필요한 약물의 양은 경구 투여로 인해 섭취하는 양에 비해 현저히 감소한다. 둘째, 약물을 지속적으로 방출하며, 약물의 효과가 더 오래 지속된다. 마지막으로, 염증부위로의 특이적 약물 전달은 다른 질병에 사용함에 있어 확장성이 있다. 결론적으로, 장 외벽 접착, 표적 특이적 약물전달 시스템으로 인해 사용해야하는 약물의 양을 줄이고 표적 특이전달 및 지속방출을 증가시켜 약물의 부작용을 줄일 수 있다.

핵심되는 말 : 장 외벽 접착성, 염증성 장 질환, 펩타이드 결함 하이드로겔, 온도감응성 졸-젤 전이, 편모 유래 펩타이드

PUBLICATION LIST

1. Kwon IG, Kang CW, Park J-P, Oh JH, Wang EK, **Kim TY**, et al. Serum glucose excretion after Roux-en-Y gastric bypass: a potential target for diabetes treatment. Gut 2020.
2. **Kim TY**, Kim DH, Yoon JK, Kim S, Yi SW, Oh WT, et al. External Self-Closing Tube to Occlude a Vessel Gradually as a Therapeutic Means of Portosystemic Shunt. Advanced Therapeutics:2000039.